

Force-Based Interaction for Distributed Precision Assembly

Richard T. DeLuca, Alfred A. Rizzi, and Ralph L. Hollis
The Robotics Institute, Carnegie Mellon University
Pittsburgh, USA
{delucr,arizzi,rhollis}@ri.cmu.edu

Abstract: This paper documents our efforts to instantiate force-guided cooperative behaviors between robotic agents in the *minifactory* environment. Minifactory incorporates high-precision 2-DOF robotic agents to perform micron-level precision 4-DOF assembly tasks. Here we utilize two minifactory agents to perform compliant insertion. We present a custom force sensing device which has been developed as well as the control and communication systems used to coordinate the action of the agents. Finally, we conclude by presenting a set of experimental results which document the performance of the new force sensor as integrated in the minifactory system. These results document the first experimental confirmation of high-bandwidth (> 100 Hz) coordination between agents within the minifactory system.

1. Introduction

In the Microdynamic Systems Laboratory¹ we are developing a class of precision automated assembly systems based on collections of low-degree-of-freedom robots. These independent robotic devices (termed *agents*) each possess a set of actuators and sensors along with a control system and communications facilities to enable cooperative action [1, 2]. This collection of robotic agents forms *minifactory* – a high-precision, self-calibrating, agent based, distributed assembly system. It is a physical instantiation of a much broader philosophy for precision assembly systems called the Agile Assembly Architecture (AAA). The motivation behind AAA and the minifactory is to create a new standard for rapidly deployable automatic assembly systems capable of precision assembly of complex electro-mechanical products [3]. Developing and deploying suitably precise and flexible sensing capabilities on the individual robotic agents is critical to reach the level of inter-agent coordination necessary to achieve this goal. Toward this end our research group recently reported on the application of frame-rate visual sensing for inter-agent coordination within the minifactory [4]. This paper complements that earlier work and focuses on the development of force-based interaction strategies for coordinating minifactory agents.

The use of force sensors to enable the performance of contact tasks is a well-studied topic. The work presented here builds directly on many earlier efforts – most notably the work by Mason [5], Craig and Raibert [6], Hogan [7], Anderson and Spong [8], Khatib [9], and Siciliano [10]. Our challenge is to map these ideas effectively onto a flexible distributed automated assembly

¹See <http://www.cs.cmu.edu/~msl>.

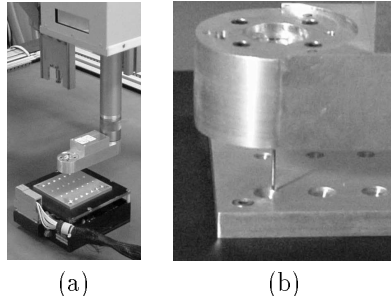


Figure 1. (a) View of courier (lower robot), configured for an insertion task, collaborating with an overhead manipulator (upper robot). (b) Close up view of the manipulator’s end effector preparing to insert a peg into a hole.

system. The resulting control methodologies (described in Sec. 3.1) most closely resemble the class of impedance controllers originally proposed by Hogan.

The remainder of this paper describes the development of a force-based coordination strategy for the two major classes of agents in the minifactory system (couriers and manipulators). To achieve this level of inter-agent coordination requires deployment of both a suitable sensing system and a distributed control system. We document the design, implementation, deployment and experimental results obtained from force-sensing hardware designed expressly for distributed force-based assembly tasks and go on to detail the communication and control strategies required to coordinate the actions of two agents cooperatively performing such a task. Section 2 briefly describes the available minifactory infrastructure and the specific force sensor developed for this task. Section 3 documents the details of our distributed control system and presents experimental verification of its performance.

2. Force-Based Inter-Agent Coordination

To explore the applicability of force guided coordination in the minifactory environment, we have chosen to undertake a collection of insertion (“peg-in-hole”) tasks. Briefly, the minifactory system (used to perform the experiments presented in this paper) uses two classes of robotic agents to perform automated assembly[1, 3]. The first class (courier agents) provides motion in the x, y plane – both translation and a limited range of rotation. It incorporates a magnetic position sensor device, providing $0.2 \mu\text{m}$ resolution (1σ) position measurements [11] and closed loop position control [12]. The second class (manipulator agents) provides vertical (z) and rotational (θ) movement. Motion resolution in z is approximately $2 \mu\text{m}$, while resolution in θ is roughly 0.0005° . Our sample task requires the cooperative application of both types of agents: a courier to carry a plate bearing a chamfered hole, and a manipulator that will measure forces on a peg as it is inserted into the hole. By exchanging state, sensor, and command information between the two agents they will act as a single 4-DOF device to reliably perform the insertion task.

2.1. Communications Infrastructure

To facilitate cooperation between physically distinct agents in the minifactory, each agent is equipped with two 100 Mb Ethernet network interface devices.

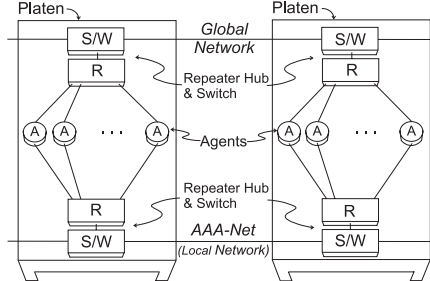


Figure 2. Physical network structure.

The first network carries non-latency-critical information, such as user commands or monitoring information – this network utilizes standard IP protocols. The second network (referred to as AAA-Net) carries real-time information critical to the timely coordination of activity between agents. This includes commands, state, and sensor information shared between the agents while performing the coordinated activities described in Section 3.

Fig. 2 depicts the physical communications infrastructure of the minifactory system. As can be seen, both the AAA-Net and the global IP network are configured as a chain-of-star topology local-networks, with a Fast Ethernet hub at the center of each star and Fast Ethernet switches forming the connections between the local-network segments. The switches serve to localize communications within the factory system by not transmitting data packets destined for local agents to the remainder of the factory and by selectively transmitting those packets destined for other network segments toward their destination, yielding a scalable communications infrastructure². A more detailed description of the protocols used by this network and the resulting system performance can be found in [4] and [13].

2.2. Integrated 3-DOF Force Sensor

While there exists a wide selection of commercially available force sensors, the minifactory application presents several significant design constraints that led us to choose to fabricate a new force sensor. Precision assembly involving small parts requires small force resolution. The force sensor was designed such that manipulation devices could be interchanged easily and packaged such that vision, manipulation, and force sensing are integrated. The resulting sensor is capable of measuring two lateral moments and the applied force. It is packaged within the end effector of the manipulator agent which in turn directly interfaces with the manipulator through a single modular connector.

2.2.1. Sensor Design

The majority of applications under consideration for minifactory utilize vertical insertion assembly and single point vacuum gripping, making a three-axis force sensor sufficient. The sensor measures force along the z axis and torques about the x and y axes. Fig. 3(a) shows an assembly view of the CAD model for the

²Note that in AAA/minifactory the bulk of high-bandwidth communication will be between agents that are attached to the same network segment, while the remainder will involve agents that are typically attached to neighboring segments [3].

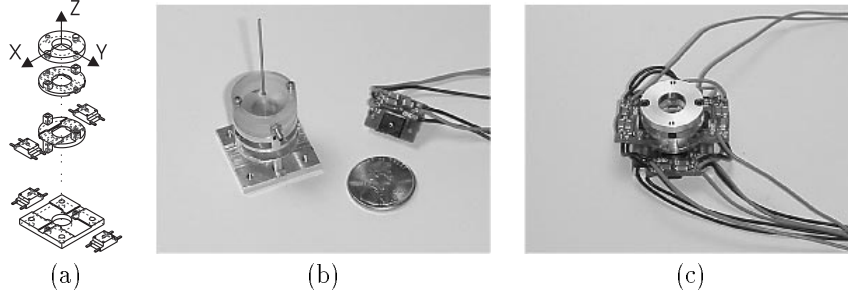


Figure 3. 3-Axis force sensor: (a) exploded assembly drawing of the flexure and single-axis load cells, (b) photograph of the flexure with clear LexanTM vacuum chamber and one load cell, (c) flexure with four load cells in place.

sensor. The sensor was designed to provide sensitivity of at least 0.1 N, minimal hysteresis, and a force range of several Newtons. A wide range of sensing modalities were considered, including semiconductor and foil strain gauges, as well as capacitive, inductive, piezoelectric, and optical elements. The final design (shown in Fig. 3(b) and (c)) utilizes a set of four commercial single-axis piezoresistive load cells (Cooper Instruments LPM-562) in a mechanical flexure. The result is a low-cost, thermally stable, easily manufactured device.

The applied force and moments are transmitted to the four load cells through a flexure. Linear analysis of the flexure yields a model relating applied forces and moments to load cell readings of the form

$$\begin{bmatrix} V_1 \\ V_2 \\ V_3 \\ V_4 \end{bmatrix} = \underbrace{\begin{bmatrix} \frac{\alpha_1}{\beta_1} & \frac{\epsilon_1}{\beta_1} & 0 \\ \frac{\alpha_2}{\beta_2} & \frac{\epsilon_2}{\beta_2} & 0 \\ \frac{\eta_1}{\delta_1} & 0 & \frac{\zeta_1}{\delta_1} \\ \frac{\eta_2}{\delta_2} & 0 & \frac{\zeta_2}{\delta_2} \end{bmatrix}}_C \begin{bmatrix} F \\ M_x \\ M_y \end{bmatrix}, \quad (1)$$

where F , M_x , and M_y represent the applied force and moments respectively, while V_i represents the measured load cell voltages. This linear representation models the flexure as cantilever beams and the load cells as stiff springs. Ideally, if the load cells are symmetrically arranged within the flexure it will be the case that $\alpha_1 = \alpha_2$, $\beta_1 = \beta_2$, $\epsilon_1 = -\epsilon_2$, $\eta_1 = \eta_2$, $\delta_1 = \delta_2$, and $\zeta_1 = -\zeta_2$, leaving only four unknown parameters required to characterize the sensor.

2.2.2. Calibration

Our prototype force sensor was calibrated to both validate this model and to determine the appropriate parameters for our device as built. To accomplish this, the force sensor was mounted in the end effector and fitted with a flat plate. Forces ranging up to 2 N were applied at 49 points evenly spaced over the entire plate. Linear regression was performed on the resulting data to produce an estimate of the matrix C ,

$$\hat{C} = \begin{bmatrix} 0.594 & -121 & -9.66 \\ 0.791 & 129 & -5.31 \\ 0.0804 & -3.44 & 120 \\ 0.184 & -9.56 & -82.1 \end{bmatrix}.$$

The absence of the expected zero elements and the lack of symmetry can be attributed to fabrication and assembly inaccuracies including load cell placement and machining tolerances. In particular, lateral displacement of the load cells was not considered in the idealized model. Based on this calibration of the sensor and observed noise properties of the sensing elements, we conclude that this force sensor is capable of resolving forces down to roughly 24 mN (1σ) and torques of approximately $0.13 \text{ mN} \cdot \text{m}$ (1σ).

3. Experimental Evaluation

We have undertaken a number of experiments to evaluate the performance of the distributed agent pair performing an insertion task. In order to accomplish this, we developed a control architecture which minimizes inter-agent communication by making use of algorithmically simple control schemes. Impedance control provides one such simple class of control policies and accomplishes stable interaction with an environment by converting the system to a form which naturally performs the task.

3.1. Control Architecture

To deploy an impedance control scheme we begin by specifying the desired behavior of the system. Given a desired mass (M_d), stiffness (K_d), damping (B_d), and force (F_d) the desired system behavior is given by

$$M_d \ddot{q} + K_d(q - q_0) + B_d \dot{q} + G_i \int_0^t (F_e - F_d) d\tau = F_e, \quad (2)$$

where q represents the generalized configuration of the system and F_e the applied environmental force acting on the system. This system behaves like a mass attached to a spring and damper about a nominal target q_0 , with the added integral term driving the system to the desired contact forces (F_d).

To realize the behavior defined by (2) we developed distributed control policies for the two independent robotic agents. The courier can be modeled as a mass with essentially ideal actuators in the x and y directions. This is a direct result of the simple actuator mechanism and the frictionless nature of the air bearing that supports the courier [12, 14]. The overhead manipulator's θ axis is directly driven, resulting in negligible friction and an equally simple model. The z axis is driven by a ball screw so a friction term was included to offset the effects of friction in that axis. Thus, the dynamic model of the system takes the form

$$M_a \ddot{q} + B_a \dot{q} + f(\dot{q}) = \tau_a - F_e, \quad (3)$$

where M_a and B_a are 4×4 diagonal matrices that describe the overhead manipulator's and courier's mass and damping parameters; $f(\dot{q})$ contains the friction terms; τ_a represents the applied actuator forces; and F_e is the applied environmental forces. It is this last term that will be measured by the force sensor mounted on the manipulator's end effector described in Section 2.2.

Given the system model and desired impedance, applying inverse dynamics yields a control law of the form

$$\tau_a = M_a M_d^{-1} \left[F_e + K_d(q_0 - q) - B_d \dot{q} + G_i \int_0^t (F_e - F_d) d\tau \right] + B_a \dot{q} + f(\dot{q}) + F_e. \quad (4)$$

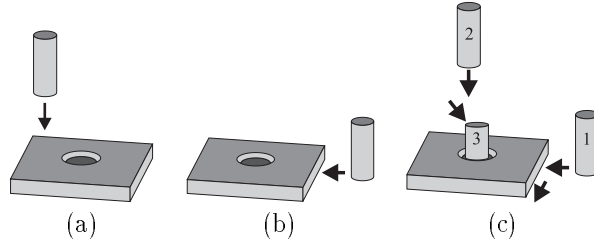


Figure 4. Graphic depiction of the three classes of experiments performed: (a) vertical contact, (b) lateral contact, and (c) peg-in-hole.

This control law is implemented separately on the two agents, with each agent responsible for its actuated degrees of freedom. By choosing to only allow diagonal matrices for M_d , K_d , B_d , and G_i this control policy is completely diagonal, which implies that the only information that must be shared between the agents are the sensed environmental forces.

Critical to implementing the above control law is the communication infrastructure described in Section 2.1. Messages sent to the courier from the overhead manipulator at real-time rates (roughly 500 Hz) contain force sensor information, velocity commands, and controller mode. The velocity commands and controller mode information allow the manipulator agent to command a variety of different behaviors from the courier agent.

3.2. Experimental Results

In the experiments described, the overhead manipulator performs contact tasks with a 0.813 mm (0.032 in.) diameter hypodermic tube attached to the force sensor (see Fig. 1(b) and 3(b)). Mounted on the courier is a plate containing several sets of holes 6.35 mm (0.25 in.) in depth and ranging in diameter from 2.54 mm (0.1 in.) to 0.838 mm (0.033 in.) (see Fig. 1). Each hole has a 45° chamfer.

Three types of tasks were performed to characterize overall system performance; vertical contact, lateral contact, and peg-in-hole insertions (see Fig. 4). Additionally, repeatability and reliability experiments were performed to verify overall system performance.

3.2.1. Vertical Contact

The vertical contact experiment involved the courier maintaining a fixed position while the overhead manipulator makes contact and maintains a constant force with the plate. Specifically, the courier performs a move (under position control) to place it under the manipulator and holds its position. Meanwhile, the manipulator finds the top of the plate on the courier by executing a constant velocity, force-guarded move. With the exact position of the plate top registered, the manipulator servos to a z position above the plate by a height equal to the depth of a hole. Once the tool tip has arrived at this position, an impedance controller is activated with the desired position located appropriately below the surface of the plate to obtain the desired contact force at equilibrium. For this experiment the desired z force was -1 N. Results from a typical experiment are shown in Fig. 5. Note the slightly underdamped response of the z force and the steady state value of -1 N. The observed high

frequency noise in the force information is attributed to unmodeled dynamics in the gripper tube. The settling time from impact is approximately 1 s. Response rates faster than this were difficult to achieve without higher impact forces. Friction in z appears to be the limiting factor.

3.2.2. Lateral Contact

The goal of the lateral contact experiment is to position the tool tip below the plane of the top of the plate while the courier makes contact and maintains a constant lateral force with the side of the plate. The top of the plate is located with a constant velocity, force-guarded move as in the vertical contact experiment. Controllers are then deployed to reposition the courier and bring it into lateral contact with the tool tip. When contact is made, the manipulator executes an impedance controller which in turn issues desired position commands to the courier controller. The desired contact force was set to -0.4 N in y . Results of a typical experiment can be found in Fig. 6. Notice that the force applied in the y direction reaches a steady state value of -0.4 N . A non-zero steady state value for the x force can be attributed to small misalignments of the gripper tube, misalignments of the courier plate, or compliance in the manipulator's θ axis. The observed settling time is roughly 0.3 s. It is expected that faster settling times can be achieved for lateral contact in which the stiffness of the θ axis of the manipulator is increased.

3.2.3. Peg-In-Hole

The peg-in-hole experiment consists of the courier bumping into and sliding along the manipulator gripper to register the plate corner and thus the entire plate geometry relative to the manipulator's tool tip. The initial bump and slide maneuver involves a hybrid position/force control sequence implemented through the use of the described impedance controllers. Once lateral contact is made, the manipulator commands a velocity and a mode change to the courier such that it maintains a constant force and slides along the plate edge. When the courier loses contact with the gripper, the courier's position is noted immediately and the plate geometry is registered to determine the location of the hole in tool tip coordinates. The plate top location is then calibrated as described earlier and the courier is positioned so that the gripper is directly over a chamfer of a hole. The manipulator servos to a position at the height of the plate top at which point an impedance controller activates with a desired position located at the center and appropriately below the bottom of the hole.

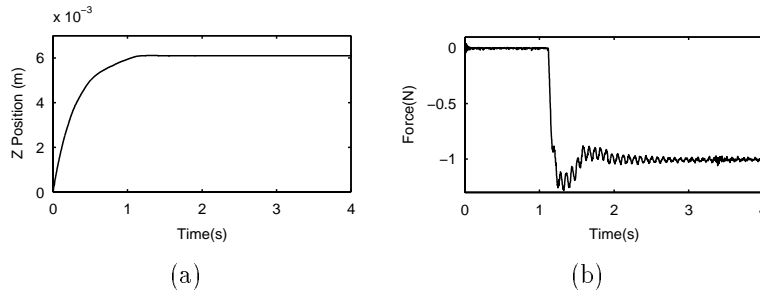


Figure 5. Position (a) and force (b) measurements during vertical contact.

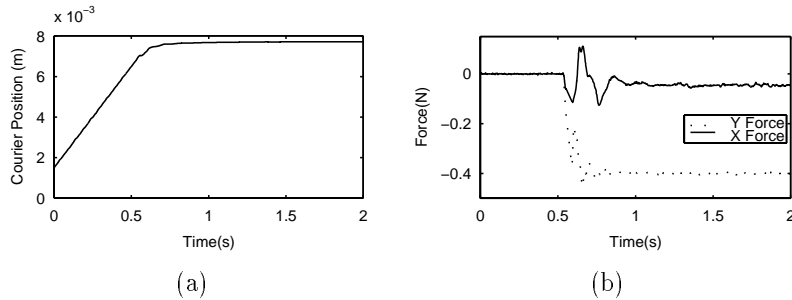


Figure 6. Position (a) and force (b) measurements during lateral contact.

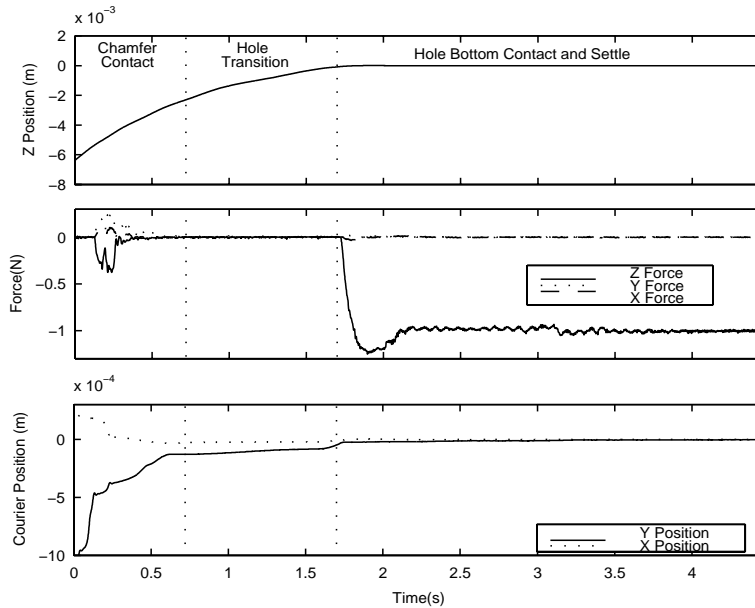


Figure 7. Overhead manipulator position, force, and courier position measurements during an insertion experiment.

The desired force is -1 N in z and 0 N in x and y . Fig. 7 shows typical results for this type of experiment. The insertion data presented is from an insertion performed on a hole with an exaggerated chamfer of diameter 6.35 mm (0.250 in.). The oversized chamfer was used to produce data with longer chamfer contact regions to aid in analysis. The exaggerated chamfer explains the lengthy duration of the insertion event. During chamfer contact one can see that the tool tip follows the chamfer down into the hole as the courier moves in response to the x and y forces. The settling time for the z force is comparable to that of the vertical contact experiment.

3.2.4. Repeatability

Results are presented from two repeatability tests in which insertion tasks

Hole Clearance	Ave. Time	Attempts	Success	RMS z Force Error
0.2032 mm	2.43 s	1000	100%	0.0663 N
0.0254 mm	2.36 s	1000	93%	0.1091 N

Table 1. Repeatability experiment results.

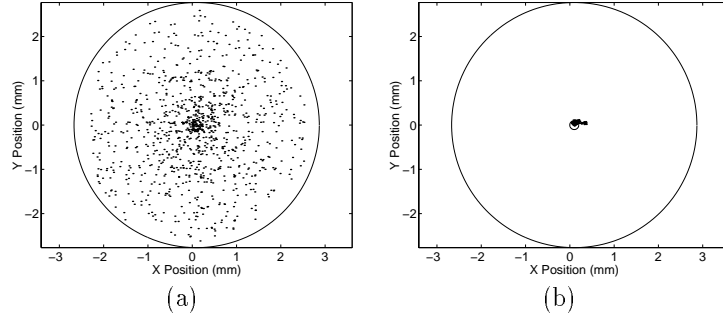


Figure 8. Tool tip start (a) and finish (b) positions plotted in configuration space for repeatability test involving a hole with 0.02032 mm (0.008 in.) clearance.

are initiated from uniformly distributed random points located above the chamfer. Repeatability was tested on a 1.016 mm (0.04 in.) hole with an exaggerated chamfer of diameter 6.35 mm (0.25 in.) and a 0.838 mm (0.033 in.) hole with a typical chamfer of diameter 1.52 mm (0.06 in.). Fig. 8 shows the start and stop positions of the tool tip in configuration space from a typical experiment. Finish positions shown outside of the hole in Fig. 8(b) are attributed to slight system miscalibration and our failure to account for small rotations of the courier. Table 1 summarizes these experiments. The difference in average insertion time is due to differences in the size of the chamfers. It is important to note that although only 93% of the 0.838 mm (0.033 in.) hole insertion attempts made it successfully into the hole, 63 of the failed attempts are attributed to system level errors. Discounting system level failures that prevented the experiment from beginning, the overall success rate rises to 99.3% for the 0.838 mm (0.033 in.) holes. Smaller clearance holes present a higher chance of wedging, which explains the larger RMS error in z force for the smaller clearance hole.

4. Conclusion

This paper serves to document the system-level communication, hardware, and control infrastructure used to perform force-based distributed precision assembly in the minifactory environment. A novel 3-axis force sensor design is presented for use in the prototype minifactory end effector. The force sensor incorporates compact design and suitable sensitivity for vertical insertion tasks. The performance measured from the results presented in this paper convincingly demonstrate the viability and potential of high-bandwidth cooperative manipulation tasks.

Acknowledgments

This work was supported in part by NSF grants DMI-9523156, and CDA-9503992. The authors would like to thank Arthur Quaid, Zack Butler, Jay Gowdy, Shinji Kume, Mike Chen, Ben Brown, and Patrick Muir for their invaluable work on the minifactory/AAA project and support for this paper.

References

- [1] Ralph L. Hollis and Arthur E. Quaid. An architecture for agile assembly. In *Proc. Am. Soc. of Precision Engineering, 10th Annual Mtg.*, Austin, TX, October 15-19 1995.
- [2] Alfred A. Rizzi and Ralph L. Hollis. Opportunities for increased intelligence and autonomy in robotic systems for manufacturing. In *International Symposium of Robotics Research*, pages 141-151, Hayama, Japan, October 1997.
- [3] Alfred A. Rizzi, Jay Gowdy, and Ralph L. Hollis. Agile assembly architecture: An agent-based approach to modular precision assembly systems. In *Proc. IEEE Int'l. Conf. on Robotics and Automation*, pages Vol. 2, p. 1511-1516, Albuquerque, April 1997.
- [4] Michael L. Chen, Shinji Kume, Alfred A. Rizzi, and Ralph L. Hollis. Visually guided coordination for distributed precision assembly. In *Proc. IEEE Int'l Conf. on Robotics and Automation*, pages 1651-1656, April 2000.
- [5] Matt T. Mason. Compliance and force control for computer controlled manipulators. In *IEEE Transactions on Systems, Man, and Cybernetics*, pages 418-432, June 1981.
- [6] Marc H. Raibert and John J. Craig. Hybrid position/force control of manipulators. In *Journal of Dynamic Systems, Measurement, and Control*, pages 126-133, 1981.
- [7] Neville Hogan. Impedance control: An approach to manipulation: Part i - theory, part ii - implementation, part iii - applications. In *Journal of Dynamic Systems, Measurement, and Control*, pages 1-24, 1985.
- [8] Robert J. Anderson and Mark. W. Spong. Hybrid impedance control of robotic manipulators. In *IEEE Journal of Robotics and Automation*, pages 549-556, Oct 1988.
- [9] Oussama Khatib. A unified approach for motion and force control of robot manipulators: The operational space formulation. In *IEEE Journal of Robotics and Automation*, pages 43-53, Feb 1987.
- [10] Stefano Chiaverini, Bruno Siciliano, and Luigi Villani. A survey of robot interaction control schemes with experimental comparison. In *IEEE Transactions on Mechatronics*, pages 273-285, Sept 1999.
- [11] Zack J. Butler, Alfred A. Rizzi, and Ralph L. Hollis. Precision integrated 3-DOF position sensor for planar linear motors. In *Proc. IEEE Int'l. Conf. on Robotics and Automation*, pages 3109-14, 1998.
- [12] Arthur E. Quaid and Ralph L. Hollis. 3-DOF closed-loop control for planar linear motors. In *Proc. IEEE Int'l Conf. on Robotics and Automation*, pages 2488-2493, May 1998.
- [13] Shinji Kume and Alfred A. Rizzi. A high-performance network infrastructure and protocols for distributed automation. In *Proc. IEEE Int'l Conf. on Robotics and Automation*, 2001. (to appear).
- [14] Bruce A. Sawyer. Linear magnetic drive system. U. S. Patent 3,735,231, May 22 1973.